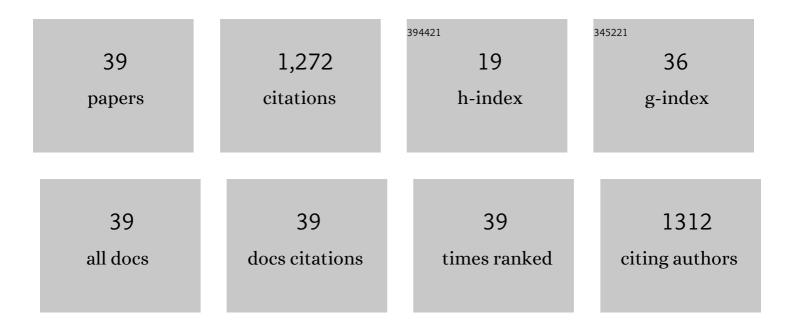
Takumi Kikegawa

List of Publications by Year in descending order

Source: https://exaly.com/author-pdf/1536774/publications.pdf Version: 2024-02-01



#	Article	IF	CITATIONS
1	In situ determination of the phase boundary between Wadsleyite and Ringwoodite in Mg2SiO4. Geophysical Research Letters, 2000, 27, 803-806.	4.0	121
2	Aluminous hydrous mineral <i>δ</i> â€AlOOH as a carrier of hydrogen into the coreâ€mantle boundary. Geophysical Research Letters, 2008, 35, .	4.0	103
3	Exploratory studies of silicate melt structure at high pressures and temperatures by in situ X-ray diffraction. Journal of Geophysical Research, 2004, 109, .	3.3	78
4	Fe-Mg partitioning between (Mg, Fe)SiO3post-perovskite, perovskite, and magnesiowüstite in the Earth's lower mantle. Geophysical Research Letters, 2005, 32, n/a-n/a.	4.0	77
5	Plagioclase breakdown as an indicator for shock conditions of meteorites. Nature Geoscience, 2010, 3, 41-45.	12.9	71
6	The stability and equation of state for the cotunnite phase of TiO2 up to 70ÂGPa. Physics and Chemistry of Minerals, 2010, 37, 129-136.	0.8	60
7	Compression of iron hydride to 80 GPa and hydrogen in the Earth's inner core. Geophysical Research Letters, 2004, 31, n/a-n/a.	4.0	59
8	Interaction between iron and post-perovskite at core-mantle boundary and core signature in plume source region. Geophysical Research Letters, 2006, 33, .	4.0	59
9	Iron-water reaction at high pressure and temperature, and hydrogen transport into the core. Physics and Chemistry of Minerals, 2005, 32, 77-82.	0.8	56
10	Stability of the Liquid State of Imidazolium-Based Ionic Liquids under High Pressure at Room Temperature. Journal of Physical Chemistry B, 2015, 119, 8146-8153.	2.6	56
11	In situ X-ray observation of the reaction dolomite = aragonite + magnesite at 900–1300 K. American Mineralogist, 2002, 87, 922-930.	1.9	53
12	Dislocation-accommodated grain boundary sliding as the major deformation mechanism of olivine in the Earth's upper mantle. Science Advances, 2015, 1, e1500360.	10.3	49
13	In situ X-ray observation of decomposition of superhydrous phase B at high pressure and temperature. Geophysical Research Letters, 2003, 30, .	4.0	43
14	Fe-Mg partitioning between perovskite and ferropericlase in the lower mantle. American Mineralogist, 2009, 94, 921-925.	1.9	42
15	Melting of iron–silicon alloy up to the core–mantle boundary pressure: implications to the thermal structure of the Earth's core. Physics and Chemistry of Minerals, 2010, 37, 353-359.	0.8	41
16	Thermal equation of state of omphacite. American Mineralogist, 2003, 88, 80-86.	1.9	34
17	Partitioning of potassium between iron and silicate at the core-mantle boundary. Geophysical Research Letters, 2006, 33, .	4.0	27
18	In situ X-ray experiment on the structure of hydrous Mg-silicate melt under high pressure and high temperature. Geophysical Research Letters, 2007, 34, .	4.0	24

#	Article	IF	CITATIONS
19	Time-resolved X-ray diffraction analysis of the experimental dehydration of serpentine at high pressure. Journal of Mineralogical and Petrological Sciences, 2009, 104, 105-109.	0.9	24

Formation of metastable cubic-perovskite in high-pressure phase transformation of Ca(Mg, Fe,) Tj ETQq0 0 0 rgBT /Overlock 10 Tf 50 70

21	Effect of incorporation of iron and aluminum on the thermoelastic properties of magnesium silicate perovskite. Physics and Chemistry of Minerals, 2007, 34, 131-143.	0.8	17
22	Superplasticity in hydrous melt-bearing dunite: Implications for shear localization in Earth's upper mantle. Earth and Planetary Science Letters, 2012, 335-336, 59-71.	4.4	17
23	Decarbonation and melting in MgCO ₃ –SiO ₂ system at high temperature and high pressure. Journal of Mineralogical and Petrological Sciences, 2015, 110, 179-188.	0.9	17
24	Compressibility of phase Egg AlSiO ₃ OH: Equation of state and role of water at high pressure. American Mineralogist, 2003, 88, 1408-1411.	1.9	16
25	X-ray diffraction study of high pressure transition in InOOH. Journal of Mineralogical and Petrological Sciences, 2008, 103, 152-155.	0.9	15
26	In situ observation and determination of liquid immiscibility in the Feâ€Oâ€ S melt at 3 GPa using a synchrotron Xâ€ray radiographic technique. Geophysical Research Letters, 2007, 34, .	4.0	14
27	Rheology of fineâ€grained forsterite aggregate at deep upper mantle conditions. Journal of Geophysical Research: Solid Earth, 2014, 119, 253-273.	3.4	14
28	Phase Transitions in CsH 2 PO 4 Under High Pressure. Ferroelectrics, 2003, 285, 83-89.	0.6	13
29	Stability and bulk modulus of Ni3S, a new nickel sulfur compound, and the melting relations of the system Ni-NiS up to 10 GPa. American Mineralogist, 2011, 96, 558-565.	1.9	13
30	A simple opposed-anvil apparatus for high pressure and temperature experiments above 10 GPa. High Pressure Research, 2011, 31, 592-602.	1.2	7
31	Deformation cubic anvil press and stress and strain measurements using monochromatic X-rays at high pressure and high temperature. High Pressure Research, 2011, 31, 399-406.	1.2	7
32	New antiferromagnetic order with pressure-induced superconductivity in <mml:math xmlns:mml="http://www.w3.org/1998/Math/MathML"> <mml:mrow> <mml:msub> <mml:mi>EuFe</mml:mi> <mm Physical Review B, 2018, 98, .</mm </mml:msub></mml:mrow></mml:math 	ll:mana2 </td <td>nmd:mn><,</td>	nm d: mn><,
33	Density and seismic velocities of chromitite body in oceanic mantle peridotite. American Mineralogist, 2010, 95, 1422-1428.	1.9	5
34	P-V-T equation of state of hydrous phase A up to 10.5 GPa. American Mineralogist, 2021, 106, 1-6.	1.9	4
35	Thermal equation of state of lawsonite up to 10 GPa and 973 K. Journal of Mineralogical and Petrological Sciences, 2015, 110, 235-240.	0.9	3
36	Determination of Stability Filed of Delta-AlOOH Under High Pressure and Temperature. AlP Conference Proceedings, 2006, , .	0.4	2

#	Article	IF	CITATIONS
37	Pressure-Induced Phase Transition in K <i>_x</i> Fe _{2â``} <i>_y</i> S ₂ . Journal of the Physical Society of Japan, 2017, 86, 033705.	1.6	2
38	Variations of lattice constants and thermal expansion coefficients of indium at high pressure and high temperature. High Pressure Research, 2018, 38, 406-413.	1.2	2
39	Evaluation of isomer shifts via 57Fe nuclear forward scattering technique with α-Fe under external magnetic field. Hyperfine Interactions, 2020, 241, 1.	0.5	Ο